GBF1 (Gartenzwerg)-dependent secretion is required for *Drosophila* tubulogenesis

Shuoshuo Wang[1], Heiko Meyer[1], Amanda Ochoa-Espinosa[2], Ulf Buchwald[3], Susanne Önel[4], Benjamin Altenhein[5], Jürgen J. Heinisch[3], Markus Affolter[2] and Achim Paululat[1,*]

[1]Department of Biology, University of Osnabrück, Zoology/Developmental Biology, Barbarastraße 11, D-49069 Osnabrück, Germany
[2]Biozentrum of the University of Basel, Klingelbergstraße 70, CH-4056 Basel, Switzerland
[3]Department of Biology, University of Osnabrück, Genetics, Barbarastraße 11, D-49069 Osnabrück, Germany
[4]Philipps-Universität Marburg, Fachbereich Biologie, Entwicklungsbiologie, D-35043 Marburg, Germany
[5]Johannes-Gutenberg Universität Mainz, Institut für Genetik, J.-J. Becherweg 32, D-55099 Mainz, Germany
*Author for correspondence (paululat@biologie.uni-osnabrueck.de)

Accepted 16 August 2011
Journal of Cell Science 125, 461–472

doi: 10.1242/jcs.092551

Summary

Here we report on the generation and in vivo analysis of a series of loss-of-function mutants for the *Drosophila* ArfGEF, Gartenzwerg. The *Drosophila* gene *gartenzwerg* (*garz*) encodes the orthologue of mammalian GBF1. *garz* is expressed ubiquitously in embryos with substantially higher abundance in cells forming diverse tubular structures such as salivary glands, trachea, proventriculus or hindgut. In the absence of functional Garz protein, the integrity of the Golgi complex is impaired. As a result, both vesicle transport of cargo proteins and directed apical membrane delivery are severely disrupted. Dysfunction of the Arf1–COPI machinery caused by a loss of Garz leads to perturbations in establishing a polarized epithelial architecture of tubular organs. Furthermore, insufficient apical transport of proteins and other membrane components causes incomplete luminal diameter expansion and deficiencies in extracellular matrix assembly. The fact that homologues of Garz are present in every annotated metazoan genome indicates that secretion processes mediated by the GBF-type ArfGEFs play a universal role in animal development.

Key words: ADP-ribosylation factor (Arf), COPI, Extracellular matrix (ECM), Guanine nucleotide exchange factor (GEF), Intracellular trafficking, Lipid homeostasis, Secretory pathway, Tubulogenesis

Introduction

Tube formation in multicellular organisms depends on the ability of epithelial cells to polarize and to form basal and apical membrane compartments de novo. During tube maturation, the initially narrow lumen, formed by the apical domains of one or several cells, is considerably expanded before becoming fully functional. Although tube formation and tube branching differ mechanistically between tubular organs (Andrew and Ewald, 2010; Baer et al., 2009; Bryant and Mostov, 2008; Chung and Andrew, 2008; Strilic et al., 2010), epithelial polarization is common to all systems with the orchestrated activity of the secretory pathway representing a prerequisite for polarization. In addition to the delivery of proteins to distinct membrane compartments, sorting machineries at the membrane are required that define, for example, adhesive domains to mediate cell–cell contact between lumen-forming cells and luminal membrane regions established at the luminal surface. Correspondingly, traffic from the Golgi complex to the cell surface was shown to be crucial for lumen formation. In the *Drosophila melanogaster* tracheal system, which has become an important model to study the molecular and cellular details of tubulogenesis, lack of e.g. Sec24 (also known as Stenosis and Haunted), a cargo-binding subunit of the COPII complex, causes a reduction in luminal diameter, cell flattening and incomplete cuticle assembly (Förster et al., 2010). The observed defects are cell-autonomous and the apical–basal cell polarity remains unaffected in *sec24* mutant animals. One major function of COPII is the anterograde trafficking of cargo from the ER to the Golgi, from which surface proteins are further delivered towards the cell membrane through exocytic post-Golgi compartments (Lee et al., 2004; Spang, 2009). COPI, by contrast, plays a major role in targeting and shuttling vesicles from the Golgi back to the ER for recycling purposes. Nevertheless, components of the COPI complex are also essential for the formation of epithelial tubes. Mutations in the *Drosophila* γ-COP, a central component of the tetrameric subcomplex that forms the inner layer of a COPI vesicle, result in a reduction of the luminal diameter of the trachea (Grieder et al., 2008) and salivary glands (Jayaram et al., 2008), which is another well-defined model system for studying tubulogenesis. Indeed, virtually all mutants identified so far that affect assembly or function of the COPI or COPII complexes interfere with proper tubulogenesis in multicellular organisms. ADP-ribosylation factor guanine nucleotide exchange factors (ArfGEFs) are a major class of proteins that are key regulators of intracellular vesicle trafficking. As indicated by their names, they function as guanine nucleotide exchange factors (GEFs) for Arfs and play a central role in all eukaryotic cells by controlling the activation of small monomeric G proteins (Gillingham and Munro, 2007).

Arf proteins were first identified as cofactors for cholera-toxin-A-dependent ADP ribosylation of an adenylate cyclase subunit (Kahn and Gilman, 1986). Activation of Arf1 by GTP

binding is mediated by a GBF-type (Golgi-specific Brefeldin A resistance factor) large ArfGEF. Activated Arf1 triggers the assembly of the COPI complex and other downstream effectors. Depletion, drug inhibition or RNAi-mediated knockdown of the GBF-type ArfGEF Gea1 and Gea2 in budding yeast, of GNL1 in *Arabidopsis* and of GBF1 in mammalian cell cultures, respectively, all lead to COPI dispersal and malformation of the Golgi complex. This is accompanied by a cargo-selective transport defect with a partial block of membrane protein transport from or to the ER or early Golgi. In addition, selective endocytosis is also impaired (Peyroche et al., 2001; Peyroche and Jackson, 2001; Richter et al., 2007; Sáenz et al., 2009; Szul et al., 2005; Szul et al., 2007; Teh and Moore, 2007). These findings indicate central roles of GBF-type ArfGEFs in coordinating bidirectional protein and lipid transport and in maintaining the structural integrity of the Golgi.

Systematic genome-wide searches for ArfGEFs in several genomes have led to the conclusion that GBF-type and BIG-type ArfGEF subfamilies are common to all eukaryotes (Mouratou et al., 2005). Contrary to plants and budding yeast, however, metazoan genomes possess only a single member of the GBF-type family, indicating that these proteins are not functionally redundant. The single *Drosophila* orthologue of the GBF-type ArfGEF, encoded by the gene *gartenzwerg* (*garz*; CG8487) was identified in several genome-wide gain-of-function screens. Overexpression of *garz* in neuronal tissue causes pathfinding defects of motoneurons and the formation of ectopic synaptic branches in nerves of first instar larvae (Kraut et al., 2001). Furthermore, *garz* was identified in a gain-of-function screen for genes involved in salivary gland morphogenesis. Overexpression of *garz* induces hooks in salivary glands during embryogenesis, albeit with a low level of penetrance (Maybeck and Röper, 2009). Essential functions exerted by Garz were also uncovered by RNAi-mediated genome-wide knockdown screens in *Drosophila* S2 cells for genes involved in secretion and Golgi morphogenesis. Thereby, Garz was identified as being crucial for both processes (Bard et al., 2006). A similar approach led to the confirmation of Garz as being essential for the regulation of lipid homeostasis in S2 cells (Beller et al., 2008; Guo et al., 2008). Depletion of GBF1 in mammalian HeLa cells and Garz in *Drosophila* third instar larvae salivary glands provides further evidence for a crucial role of Garz in protein trafficking and secretion (Szul et al., 2011). Recently, *garz* was identified as a regulator of the non-canonical but highly conserved GEEC (GPI–AP enriched early endosomal compartments) clathrin- and dynamin-independent endocytic pathway (Gupta et al., 2009).

We identified the ArfGEF Garz in a genetic screen for heart malformations. *garz* mutant embryos exhibit a severe defect in secretion of the type IV collagen Pericardin in pericardial cells of the circulatory system. To gain further insight into the in vivo function of Garz we generated and identified several *garz* mutant alleles. All investigated alleles cause secretion defects accompanied by malformations of the ER and the Golgi complex. In addition we found that tubulogenesis in salivary glands and trachea is severely impaired in the absence of Garz. Herein we present the first phenotypic analysis of a metazoan GBF-type ArfGEF loss-of-function mutant in an organismic context.

Results

garz is continuously expressed during *Drosophila* development with highest abundance in glandular and tubular organs

Sequence analysis revealed that the *Drosophila* genome contains a single homologue of the human ArfGEF GBF1, called Gartenzwerg (Garz). The deduced amino acid sequence of Garz shares 44% identical and 61% similar residues with its human homologue, and has all conserved domains typical for ArfGEFs of the GBF-type protein subfamily (Fig. 1A,B). We initially analyzed the temporal and spatial expression of *garz* during embryogenesis and later stages of development by in situ hybridization and northern blot analysis. A *garz* cDNA sequence present in all putative splice variants predicted by the latest *Drosophila* genome annotation was used as a template to generate specific probes. Northern blot analysis revealed that two transcripts, presumably corresponding to the predicted isoforms *garz*-RA and *garz*-RB, are expressed during development, with transcript *garz*-RB being highly abundant in all stages tested and transcript *garz*-RA being present mainly in pupae and adults, but in much lower amounts (Fig. 1C). The third predicted isoform, *garz*-RC, was not detected. Whole-mount in situ hybridization revealed that in the embryo *garz* is most prominently expressed in invaginating ectodermal derivatives during gastrulation, i.e. in the primordia of the salivary glands, the proventriculus part of the stomodeum, the hindgut part of the proctodeum and in the tracheal placodes of embryos from stage 10 to 11 (Fig. 1D–R). Expression in these tissues is maintained later in development. In addition to the strong expression of *garz* in tissues that form tubular structures of epithelial character, a weak maternal contribution and a weak ubiquitous zygotic expression is apparent.

In order to analyze the subcellular localisation of Garz, we raised polyclonal antibodies against the protein (see Materials and Methods for details). The monospecificity of the affinity purified antibodies was verified by western blot analysis using protein extracts isolated from S2 cells and from whole flies (Fig. 2A). In protein preparations from S2 cells, a single band was detected at ~220 kDa, which corresponds well to the longer Garz isoform B (predicted molecular mass: 220.64 kDa). In protein extracts isolated from flies, a protein of similar size and abundance was labelled. However, in addition to this strong signal, a weakly expressed smaller protein with an apparent molecular mass of slightly less than 200 kDa was also detected, which indicates that not only isoform B but also the putative isoform A (predicted molecular mass: 194.9 kDa) is expressed during *Drosophila* development. Western blot analysis with protein extracts from wild-type and heterozygous $garz^{\Delta 137}$, heterozygous $garz^{EMS667}$ and heterozygous $garz^{S4\text{-}50}$ animals (*garz* mutants used in this study are described in the following section) revealed a reduction in full-length Garz abundance of ~50% in the heterozygotes compared with the wild type (Fig. 2B). In agreement with these data, immunodetection showed no Garz in salivary glands of homozygous mutant *garz* embryos (Fig. 2F,H,J), which further confirms antibody specificity as well as the absence of a full-length Garz protein in these mutant alleles. To obtain initial information on the cellular compartments Garz is associated with, subcellular fractions from untransfected S2 cells were obtained by sucrose density gradient centrifugation and probed with the Garz antiserum and established markers for the *cis*-Golgi network (GM130) and early endosomes (Rab5). Rab5 was chosen because a recent publication provided evidence of a role of Garz in the endocytic

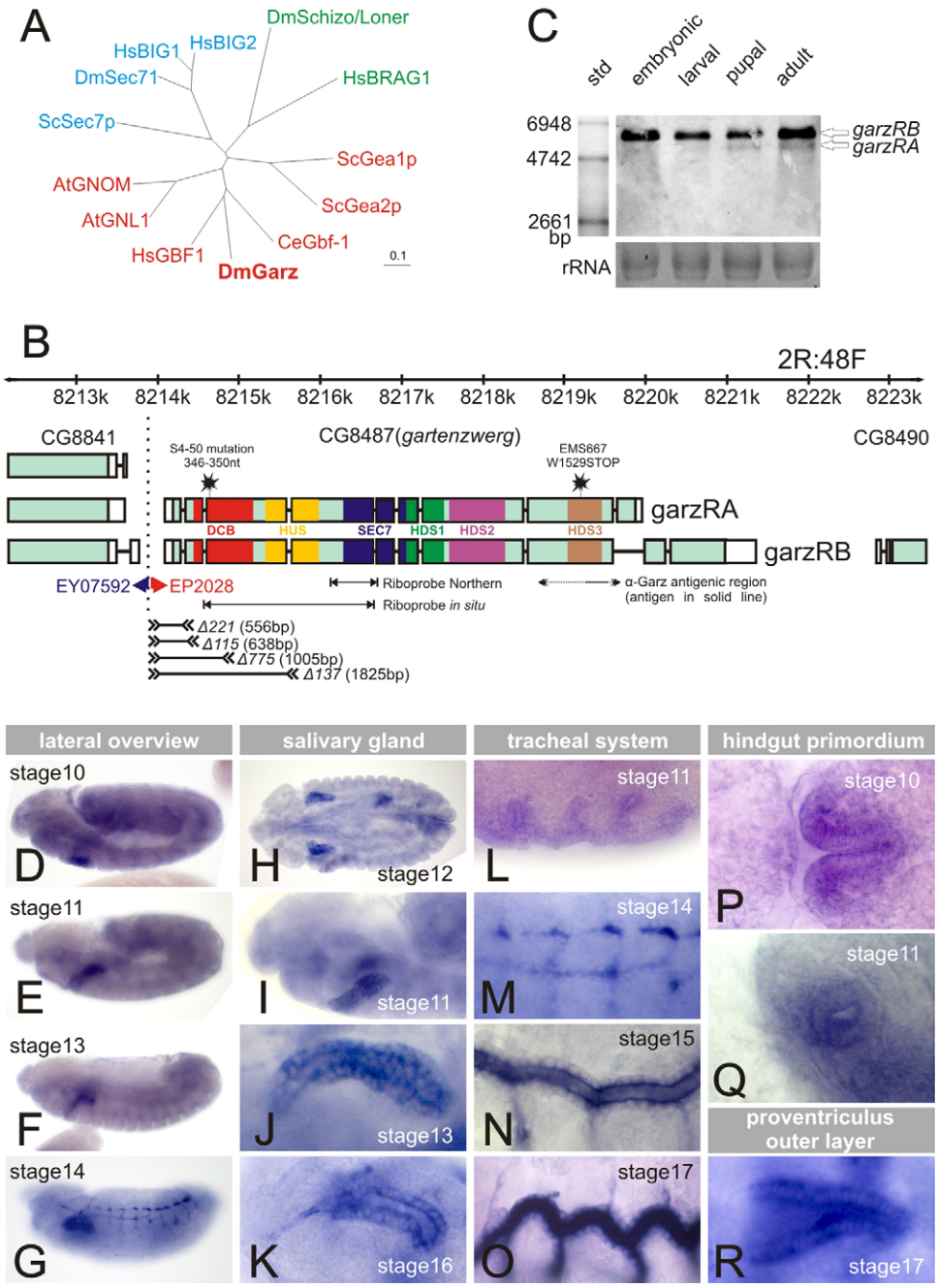

Fig. 1. ***Drosophila*** **Garz, a member of the Gbf1–GNL1–BIG-type GDP exchange factor family, is expressed at all stages of development.** (**A**) Phylogenetic analysis of selected ArfGEFs. Primary alignment was performed with ClustalX using the following sequences: AtGNL1 (NP_198766.1), AtGNOM (NP_172851.1), CeGbf1 (NP_499522.2), DmGarz (NP_610761.2), DmSec71 (NP_609675.2), DmSchizo/Loner (NP_730594.1), HsBIG1 (NP_006412.2), HsBIG2 (NP_006411.2), HsBRAG1 (NP_001104595.1), HsGBF1 (NP_004184.1), ScGea1p (NP_012565.1), ScSec7p (NP_010454.1), ScGea2p (NP010892.1). The unrooted tree was generated using the NJ (neighbour-joining) algorithm excluding gapped region and drawn with TreeView 1.6.6. The reliability of the tree was assessed by a bootstrap analysis (1000 replicates). At, *Arabidopsis thaliana*; Ce, *Caenorhabditis elegans*; Dm, *Drosophila melanogaster*; Hs, *Homo sapiens*; Sc, *Saccharomyces cerevisiae*. (**B**) Schematics of the *garz* genomic region and domain organization of Garz. Two experimentally verified isoforms (garz-RA and garz-RB) are shown. Asterisks indicate the position of the EMS-induced mutations present in $garz^{S4\text{-}50}$ and $garz^{EMS667}$. Deletions induced by imprecise excision are indicated below the schematic representation of the Garz gene. Numbers in parentheses indicate the size of the deletion. The *garz* cDNA sequences used to generate riboprobes for in situ hybridization and northern blot analysis are marked by lines with arrows. The sequence region used for heterologous expression in *E. coli* and antibody production is indicated. Epitope mapping (data not shown) revealed that the Garz antibody recognizes an epitope downstream of the stop codon present in the $garz^{EMS667}$ allele. The insertion site of the two P-elements (confirmed by sequencing) that were used in this study for complementation tests (EP2028) and jump out mutagenesis (EY07592) are marked by a blue and a red arrow. (**C**) Northern blot analysis revealed the presence of one abundant larger *garz* transcript and a second weakly expressed shorter transcript. 10 µg total RNA isolated from embryos (0–24 hours), third instar larvae, mid-stage pupae and adult flies, respectively, were blotted per lane and probed with an antisense riboprobe (see B). (**D–R**) In situ hybridization revealed a weak ubiquitous *garz* expression in wild-type embryos of *Drosophila melanogaster* and particularly strong expression in the salivary glands (H–K), in the tracheal system (L–O), in the hindgut primordia (P,Q) and in the outer layer of the proventriculus (R). Staining of the tracheal lumen in late stage embryos (O) is unspecific.

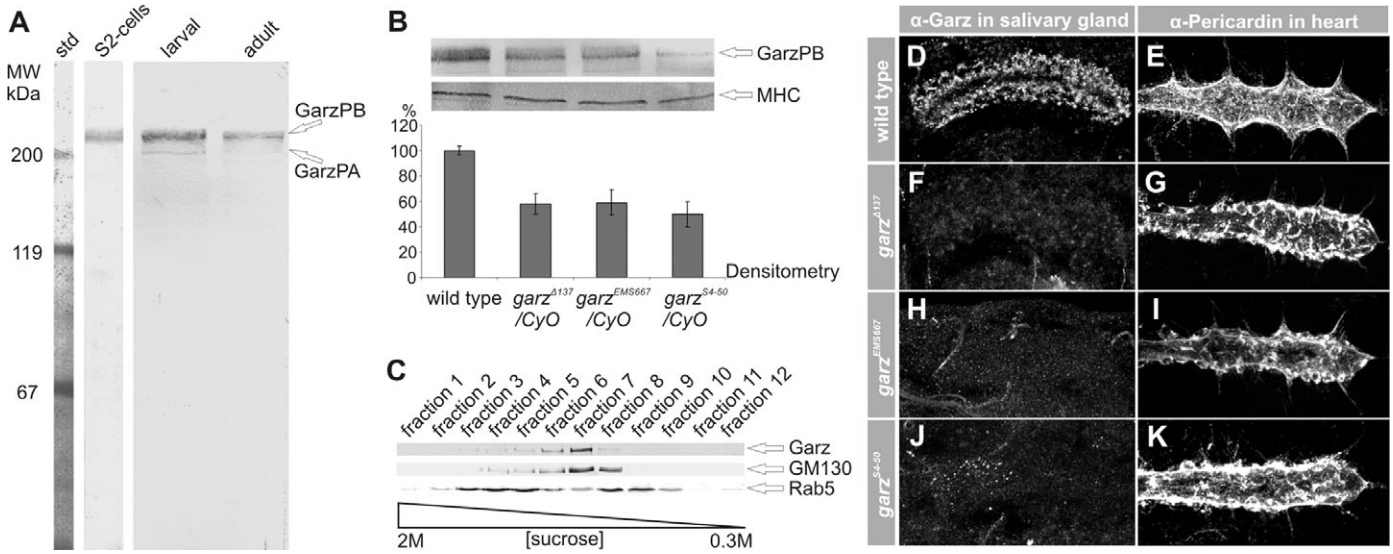

Fig. 2. Garz detection. (**A**) In western blot analyses, the affinity purified anti-Garz antibody (1:200 dilution) detects a single band of the expected molecular mass of Garz-PB in protein extracts isolated from untransfected S2 cells (left lane). In protein extracts from larvae and adult flies (middle and right lane) two bands are present that presumably correspond to the predicted isoforms Garz-PA and Garz-PB. For all samples 10 μg of protein were loaded per lane. (**B**) Protein extracts isolated from wild-type, $garz^{\Delta 137}/CyO$, $garz^{EMS667}/CyO$ and $garz^{S4\text{-}50}/CyO$ adult animals were probed with the anti-Garz antibody. As a loading control the blot was reprobed with anti-MHC (myosin heavy chain). Animals carrying one mutant *garz* allele exhibit a reduction in Garz protein of approximately 50%. The relative band intensity in relation to the loading control was assessed by densitometric analysis using a VersaDoc 4000 imaging system (Bio-Rad Laboratories, Hercules, CA, USA) and Quantity One software, version 4.6.9. The calculation was done for three independent blots. (**C**) Distribution of Garz, GM130 and Rab5 proteins in a sucrose density gradient. Postnuclear homogenates from untransfected S2 cells were fractionated on a 0.3–2.0 M linear sucrose gradient. Garz accumulates in Golgi fractions as shown by co-fractionation with the *cis*-Golgi marker GM130. The early endosomal marker Rab5 shows only a minor overlap with the distribution pattern of Garz. (**D**,**F**,**H**,**J**) Confocal micrographs of salivary glands of wild-type (D), $garz^{\Delta 137}$ (F) and $garz^{EMS667}$ (H) and $garz^{S4\text{-}50}$ (J) mutant embryos stained with anti-Garz antibody. In *garz* mutant embryos we observed no specific staining in salivary glands above background. (**E**,**G**,**I**,**K**) Confocal micrographs of the dorsal vessel of wild-type (E), $garz^{\Delta 137}$ (G) and $garz^{EMS667}$ (I) and $garz^{S4\text{-}50}$ (K) mutant embryos stained for Pericardin, a type IV collagen-like ECM protein contributing to the ECM layer that surrounds the myocardial–pericardial network. In *garz* mutant embryos Pericardin is trapped in intracellular structures and fails to be correctly incorporated into the ECM.

pathway (Gupta et al., 2009). As shown in Fig. 2C, Garz co-fractionated with *cis*-Golgi membranes as revealed by an identical distribution of Garz and GM130 with a peak accumulation in fraction 7. This result clearly indicates a function for Garz at this subcellular compartment. Rab5, however, accumulated predominately in fractions 3, 4, 5, 8 and 9, which is distinct from the distribution pattern of Garz. However, because of a certain overlap between Garz- and Rab5-positive fractions, e.g. fraction 6, an association of Garz with Rab5 endosomes cannot be excluded at this stage. To analyze Garz protein distribution in more detail, we performed colocalization studies in *Drosophila* S2 cells and in the budding yeast, *Saccharomyces cerevisiae* (Fig. 3). Simultaneous immunohistological stainings of *Drosophila* tissue with anti-Garz antibodies and for Golgi–EYFP (LaJeunesse et al., 2004) revealed that Garz is highly enriched in the ultra-proximal region of the Golgi complex, which corresponds to the *cis*-Golgi compartment (Fig. 3A–I). Clearly, Garz did not colocalize with markers for the *trans*-Golgi compartment as shown by simultaneous staining of salivary gland cells and S2 cells with anti-Garz, anti-AP1 (Benhra et al., 2011) and anti-GCC185 (Sinka et al., 2008) antibodies (Fig. 3D–F,J–O). This finding is further supported by comparing the subcellular distribution of Garz expressed in yeast cells with the localization of its yeast homologue Gea1. We found that *Drosophila* Garz and yeast Gea1 both colocalize with the yeast *cis*-Golgi marker Mnn9 (Fig. 3P–W). In summary, our results established *Drosophila* Garz as a protein of the *cis*-Golgi compartment.

Identification and generation of new *garz* mutants in *Drosophila*

We identified the S4-50 allele by screening a collection of EMS-induced mutants for heart formation defects (Albrecht et al., 2006; Hummel et al., 1999). At late stage of embryogenesis, *garz* mutant embryos show a secretion defect of the collagen Pericardin at the heart tube (Fig. 2G,I,K). The mutated gene in S4-50 was mapped by complementation analysis to chromosomal region 48F–49A on the second chromosome. S4-50 failed to complement the previously described transposon-induced *gartenzwerg* allele $garz^{EP(2)2028}$ (Rørth, 1996), in which the EP element is inserted into the putative promoter region of *garz*. A second EMS-induced *garz* allele, $garz^{EMS667}$, was isolated in the Technau laboratory (Vef et al., 2006). Transheterozygous animals with the genotype S4-50/EMS667, S4-50/EP(2)2028 or any other mutant combination are 100% lethal and show the same phenotypes as described in the following sections. To identify the EMS-induced point mutations in $garz^{S4\text{-}50}$ and $garz^{EMS667}$ mutant chromosomes we sequenced the *garz* locus from mutant animals (supplementary material Fig. S1). The $garz^{S4\text{-}50}$ chromosome carries a mutation that consists of a 2 bp deletion and the substitution of three nucleotides found in the third exon of the *garz* gene. This results in a frame shift and a premature stop codon, leading to a protein of 138 amino acids that lacks all conserved domains (supplementary material Fig. S1). The mutation in $garz^{EMS667}$ is a single G to A transition causing a premature stop codon leading to a truncated protein of 1529 amino acids. This protein lacks the C-terminus

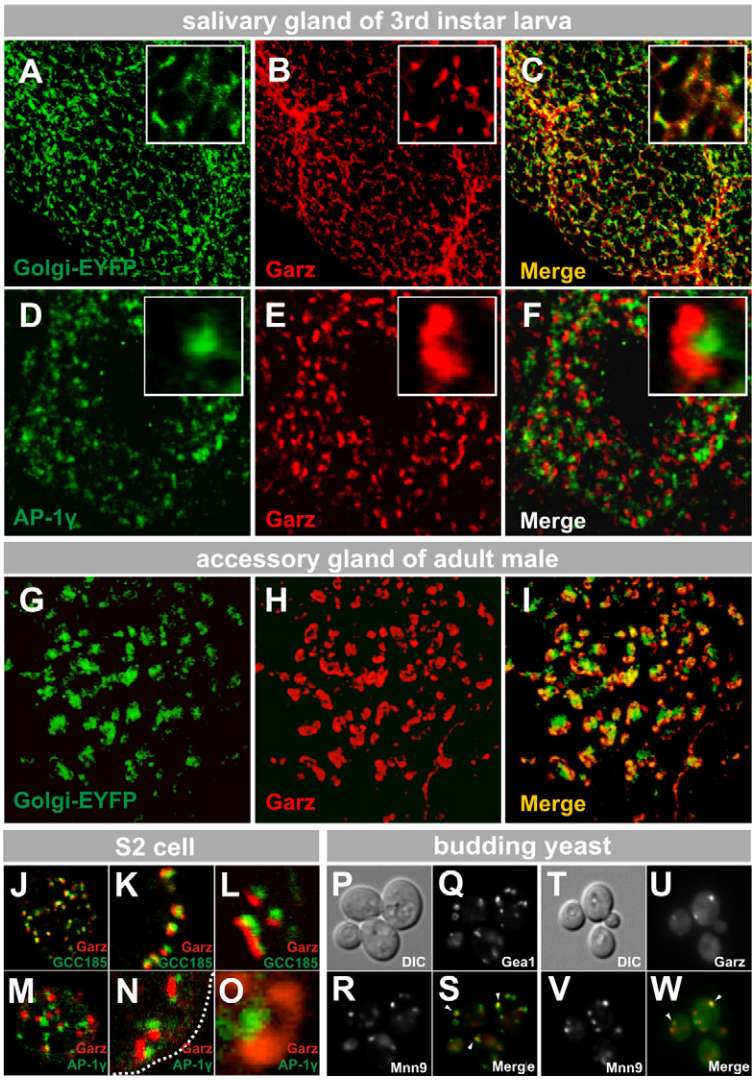

Fig. 3. Garz localizes to the *cis*-Golgi complex in *Drosophila* tissue, S2 cells and budding yeast. (**A–C**) Salivary glands from third instar larvae carrying the *sqh*::EYFP-Golgi transgene to visualize the Golgi complex (A, green channel) were stained for Garz (B, red channel). Confocal micrographs (single sections) show that Garz largely colocalizes with the Golgi marker (C, merged picture). (**D–F**) Co-staining of salivary glands from wild-type third instar larvae stained for Garz (D, green channel) and the trans-Golgi marker AP-1γ (E, red channel) indicates that Garz is excluded from the TGN (F). (**G–I**) Confocal micrographs show male accessory gland cells from adult flies stained for *sqh*::EYFP-Golgi (G, green channel) and for Garz (H, red channel). Garz localizes to distinct regions of the Golgi compartment (I). (**J–O**) Double staining of untransfected *Drosophila* S2 cells either for GCC185 (J–L) or AP-1γ (M–O) and Garz confirmed that Garz is virtually excluded from the *trans*-Golgi compartment (L). (**P–W**) *S. cerevisiae* cells were used to compare endogenous localization of the EGFP-labelled yeast homologue of Garz, Gea1 (Q) and heterologously overproduced Garz–EGFP (U), both stably integrated into the yeast genome (see Materials and Methods). As a marker for the *cis*-Golgi compartment in yeast we used td-Tomato-tagged Mnn9p (R,V). (S) Gea1 primarily exhibits a punctate staining pattern typical for Golgi-localized proteins, which partially overlaps with the signals from Mnn9-tdTomato. (W) Foci of C-terminally EGFP-tagged Garz in part colocalize with Mnn9 as well. Arrowheads indicate overlapping signals.

including the HUS3 domain (supplementary material Fig. S1). In addition, we generated a series of new *garz* deletion lines by remobilizing the transposable P-element EPgy2^{EY07592}, obtained from the Berkeley *Drosophila* gene disruption project (Bellen et al., 2004), in order to induce imprecise excision events. EPgy2^{EY07592} harbours an EP element located in the 5′-*garz* region, as we verified by sequencing. EPgy2^{EY07592} individuals are viable both as homozygotes and in trans over the deficiency Df(2R)Exel6061 that includes *garz* and several additional genes. Therefore, we considered EPgy2^{EY07592} suitable for jump-out mutagenesis and screened for lethality caused by genomic deletions as a result of imprecise excision events. The 181 lethal mutant lines that were recovered belong to two complementation groups. Further genetic and molecular characterization revealed that all alleles from one complementation group are allelic to S4-50, EMS667, EP(2)2028 and the *garz* deficiency Df(2R)Exel6061. Sequencing showed the presence of deletions ranging from 556 bp in *garz*$^{\Delta 221}$ up to 1825 bp in *garz*$^{\Delta 137}$ (Fig. 1B). In all cases the deletion breakpoints map precisely to the previous insertion site of the P-element and sequences downstream within the *garz* locus. We focused on the largest deletion present in the *garz*$^{\Delta 137}$ allele that removes the putative *garz* promoter region as well as the first exon (Fig. 1). *garz*$^{\Delta 137}$ homozygous animals develop until the end of embryogenesis but fail to hatch and subsequently die. Moreover, mutant individuals exhibit asynchronous development and considerable retardation in comparison with wild-type controls (data not shown). Similar results were obtained for *garz*$^{S4\text{-}50}$/Df(2R)Exel6061 and *garz*$^{\Delta 137}$/Df(2R)Exel6061 mutant animals, indicating that these lines represent strong *garz* alleles. Lethal phase analysis of *garz*^{EMS667}/*garz*^{EMS667}, *garz*^{EMS667}/Df(2R)Exel6061 and *garz*$^{EP(2)2028}$/*garz*$^{EP(2)2028}$ mutants revealed early first instar larval lethality with a very low number of individuals surviving until the end of larval development, which indicates that these mutants represent weaker alleles.

garz mutants have abnormal Golgi morphology that results in secretion defects in tubular structures and luminal diameter expansion

The new *Drosophila garz* alleles enabled us to study the consequences of its loss of function in a multicellular organism. This is of particular interest because until now none of the known Garz homologues from higher eukaryotes was studied in an organismic context because of the absence of mutants. Nevertheless, a crucial role of Garz in the secretory

pathway was demonstrated by biochemical analyses and studies in yeast and mammalian cell cultures (Chantalat et al., 2003; Claude et al., 1999; Niu et al., 2005; Peyroche et al., 2001; Peyroche and Jackson, 2001; Ramaen et al., 2007; Sáenz et al., 2009; Spang et al., 2001; Szul et al., 2007) and in *Drosophila* by an RNA interference (RNAi) approach (Szul et al., 2011). Recently, Gupta and colleagues also provided evidence of a role of Garz in the endocytic pathway in flies (Gupta et al., 2009). The assumed function of Garz in protein secretion suggests defects in extracellular protein deposition in *garz* mutant animals. Therefore, we stained wild-type and mutant embryos for secreted extracellular matrix (ECM) components and membrane-associated factors and focused on tissues that are known to be highly secretory. We utilized the embryonic salivary glands as a model organ to address the question of whether ECM formation at luminal membrane compartments depends, at least partially, on functional secretion and the underlying Garz activity. The second issue we were interested in was the extent to which *garz*-dependent secretion contributes to lumen diameter control in salivary glands. Staining of salivary glands with antibodies against GM130, a cytoplasmic protein tightly bound to membranes of the *cis*-Golgi network (CGN) in all higher eukaryotes (Nakamura et al., 1995), revealed that the CGN compartments of salivary gland cells were severely reduced in number in *garz* mutant embryos (Fig. 4A,B,E,F). Consistent with this observation, we found that vesicles secreting electron-dense

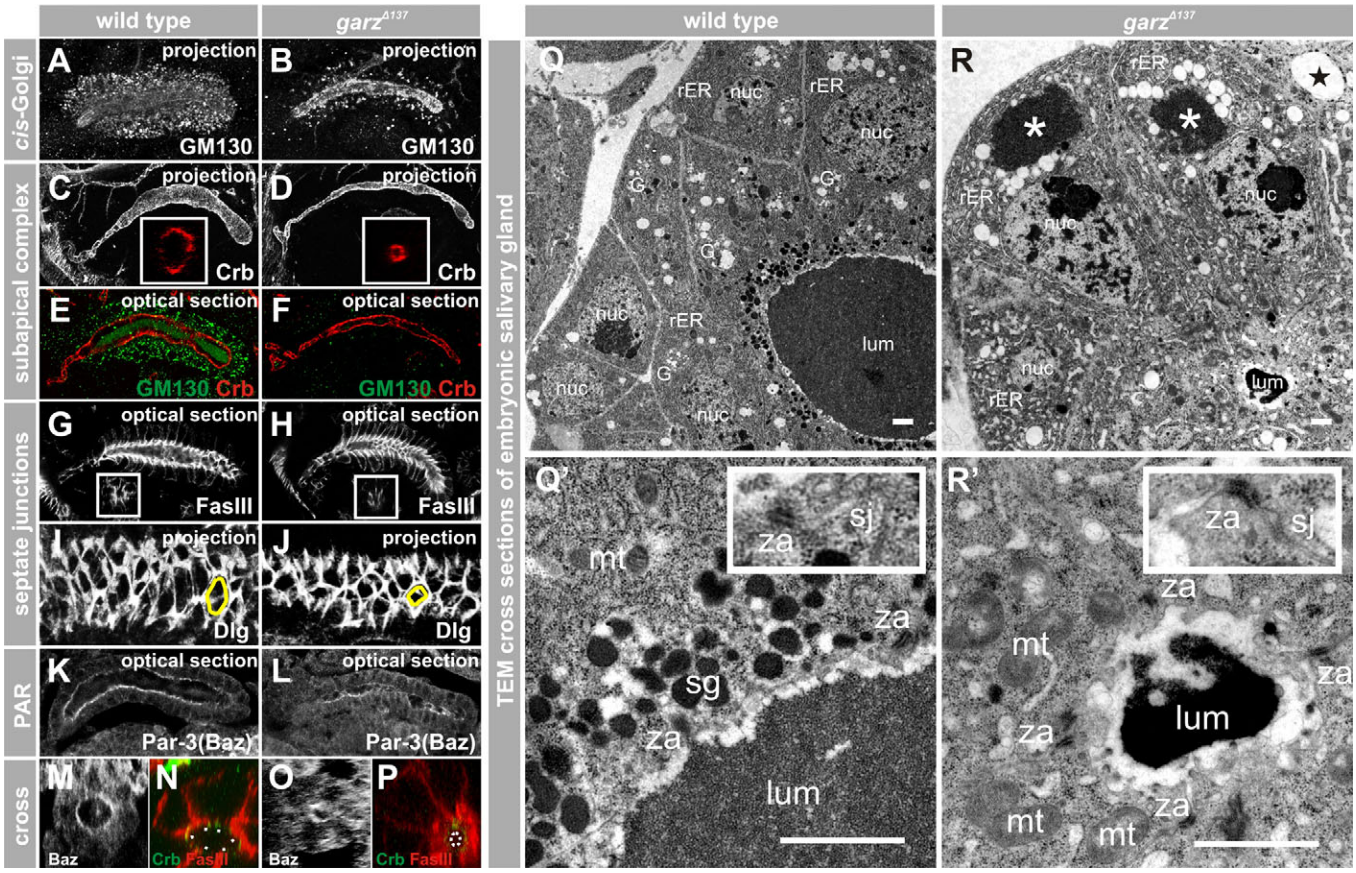

Fig. 4. Garz is required for luminal diameter expansion in embryonic salivary gland. (**A**,**B**) Confocal micrographs of wild-type salivary glands (A) and *garz*$^{\Delta 137}$ mutant embryos (B). Staining of stage 15 embryos for the Golgi marker GM130 demonstrates that Golgi morphology is severely disrupted and that the overall quantity of Golgi is reduced in *garz* mutant embryos (B) compared with wild-type embryos (A). (**C**,**D**) An antibody that recognizes Crumbs (Crb) was used to visualize the apical–luminal membranes of salivary gland cells at stage 16. Compared with wild-type glands (C), the diameter of the lumen is less in salivary glands from *garz* mutants (D). Z-projections (insets in C and D, same magnification) show the differences in the diameter in the active secretory part of the salivary glands. The diameter of the duct region remains unaffected. (**E**,**F**) Co-stainings of GM130 and Crb demonstrate the relationship between intact Golgi integrity and normal luminal diameter in wild-type (E) and *garz* mutants (F). (**G–J**) Monoclonal antibodies against Fasciclin III (FasIII; G,H) and Discs large (Dlg; I–J), both components of septate junctions, mark the basolateral membrane domains and the cell borders (I,J) between salivary gland cells. In *garz* mutants (J), the apical surface of each cell (labelled in yellow) is much smaller than in the wild type (J). (**K–P**) Bazooka (Baz) antibody was used to visualize whole salivary glands in wild-type (K) and *garz* mutants (L). (M–P) Optical cross sections of salivary glands stained for Baz show the smaller lumen diameter in *garz* (O) in comparison with wild type (M), whereas the cell size is unaffected. Staining for FasIII and Crb–GFP demonstrate specific and substantial differences of the apical domain in the wild type (N) and in *garz* mutants (P). (**Q**,**R**) TEM sections of salivary glands from wild-type (Q,Q′) and *garz* mutant stage 16 (R,R′) embryos. Numerous secretion granules (sg) accumulate at the sub-apical membrane domain in wild-type tissue (Q), whereas in *garz*$^{\Delta 137}$ (R) not only the matrix (indicated by asterisks) but also lipid droplets (adjacent white particles) accumulate at the basal side of salivary gland cells instead of being secreted into the lumen. A dilation of the ER compartment is also apparent, presumably due to protein retention. Note that both the zonula adherens and septate junctions between the four secretory cells are properly formed in *garz* mutant embryos (see insets **Q′** and **R′**). However, proper apical membrane expansion is inhibited in *garz* mutants. All scale bars: 1 µm. G, Golgi complex; lum, lumen; mt, mitochondria; nuc, nucleus; rER, rough ER; sg, secretion granules; sj, septate junction; za, zonula adherens.

ECM material, which are normally numerous close to the apical membrane of salivary gland cells at stage 16, were entirely absent in *garz* mutant embryos (Fig. 4Q,R). At the same time, the highly enriched rough ER, which is characteristic of active secretory cells, vanished in *garz* mutants. Instead, the ER compartment appeared as 'bloated balloons'. It is noteworthy that mutations in genes crucial for retrograde vesicle trafficking such as that for γ-COP, as well as anterograde vesicle trafficking such as *sec23* (also known as *ghost*) *sec24* and *sar1*, result in a very similar ER phenotype (Förster et al., 2010; Jayaram et al., 2008; Norum et al., 2010; Tsarouhas et al., 2007). Failure of luminal diameter expansion was also clearly seen by stainings for the apical membrane determinants Crumbs and Bazooka (Tepass et al., 1990; Wodarz et al., 1999) (Fig. 4C–F and insets) and in cross sections analyzed by transmission electron microscopy (TEM; Fig. 4Q,R). The formation of zonulae adherentes and septate junctions is not affected in *garz* mutant embryos, as most clearly seen in TEM sections (insets in Fig. 4Q′,R′) and in stainings for the septate junction markers Fasciclin III (FasIII) and Discs large (Dlg; Fig. 4G–J).

Taken together, our observations provide clear evidence for a specific role of Garz in luminal diameter expansion in salivary glands. Interestingly, the luminal length remains unaffected in *garz* mutant embryos (Fig. 6), indicating that Garz is not involved in invagination or in the elongation of salivary gland cells, but is involved in apical membrane expansion.

Secretion of luminal material and diameter expansion of tracheal tubes depend on *garz*

Recent studies revealed an essential role of cell–matrix interactions in tube morphogenesis, including the generation, shaping and maintenance of epithelial tubes (Affolter and Caussinus, 2008; Schottenfeld et al., 2010). Several components of the nascent tracheal lumen, e.g. the zona pellucida (ZP) protein Piopio (Pio) or the chitin deacetylases Vermiform (Verm) and Serpentine (Serp) have been shown to play essential roles in length and size control of trachea (Jazwinska et al., 2003; Luschnig et al., 2006). Furthermore, the *convoluted* gene, coding for the *Drosophila* acid-labile subunit (ALS), which forms a ternary complex with *Drosophila* insulin-like peptide 2 (Dilp2) and the binding protein IMP-L2 (Arquier et al., 2008), is required for the dynamic organization of the transient luminal matrix and for the establishment of cuticular structures that line the tracheal lumen (Swanson et al., 2009). These components are secreted from the apical membrane facing the lumen and their deposition is dependent on the secretory machinery of the cells. On the basis of our data, we assumed that Garz plays a key role in the delivery of tracheal ECM proteins to the apical membrane. Using the monoclonal antibody mAb2A12, which exclusively labels a yet unknown luminal antigen, we observed a large reduction of the tracheal luminal diameter in *garz* mutants (Fig. 5A,A′). Retention of the mAb2A12 antigen within the tracheal cells implies that loss of Garz prevents the antigen from being secreted into the lumen. We furthermore examined the distribution of the ZP protein Piopio (Bökel et al., 2005; Jazwinska et al., 2003). Piopio, which is normally secreted across the apical membrane into the luminal space and tightly linked to the ECM lining the surface of the lumen, was retained inside the cells in *garz* mutant embryos (Fig. 5B,B′). Similar results were obtained for the chitin deacetylase Vermiform (Luschnig et al., 2006) (Fig. 5C,C′). Similar to Piopio and mAb2A12, Vermiform secretion and Crumbs delivery were severely impaired in *garz* mutants. The reduction of cell matrix components at the luminal surface of trachea might also affect airway clearance. At approximately stage 17 trachea are filled with gas that has replaced the liquid present in all tracheal branches at earlier stages (Behr et al., 2007; Tsarouhas et al., 2007). In order to prove an effect of *garz* on the clearance process, we used video bright-field microscopy of living specimens and found that airways clearance was inhibited in *garz* mutant animals (Fig. 5D,D′ and supplementary material Movies 1 and 2). From this we conclude that Garz plays an important role in airway morphogenesis and maturation. Similar to our observations on salivary glands, delivery of apical membrane proteins such as Crumbs or septate junction proteins such as FasIII was not severely disturbed in tracheal cells of *garz* mutant embryos (Fig. 5E–M). Notably, before the death of homozygous *garz* mutant individuals, the tracheal lumen collapses (own observation). This might be caused by improper formation of cuticle structures that mechanically support tube stability, and such defects inside tracheal lumina should be visible in cross sections analyzed by transmission electron microscopy. As expected, besides a reduction in luminal diameter we found an aberrant organization of chitin cables inside the tracheal lumen in *garz* mutants (Fig. 5N,O). On the basis of these data, we addressed the question of whether cuticle development in general is affected in *garz*. Indeed, inspection of stage 17 embryos revealed that also epidermal secretion of the cuticle is disturbed to various degrees in *garz* mutants (supplementary material Fig. S2), which is consistent with a requirement for Garz in secretion processes mainly, but not exclusively, in tubular structures.

Discussion

During the last few years, much insight has been gained into the activities and roles of ArfGEFs using cultured mammalian cells, plants and budding yeast in conjunction with in vitro approaches. However, up to now little has been known about the physiological and developmental consequences of mutations affecting ArfGEFs of the Garz family in multicellular animals. Sheen and colleagues provided evidence that point mutations in the human *ArfGef2* (*BIG2*), identified in two patients suffering from microcephaly caused by disruption of neural precursor proliferation, inhibit protein transport from the Golgi to the cell surface (Sheen et al., 2004). A third patient with heterozygosity for two *ArfGEF2* (*BIG2*) mutations was recently reported to suffer from movement disorder, bilateral periventricular nodular heterotopia (BPNH) and secondary microcephaly (de Wit et al., 2009). However, in this case molecular data explaining these symptoms were not reported. In human HeLa cells, small-interfering RNA based suppression of ArfGEF1 (BIG1) and ArfGEF2 (BIG2), which constitute, together with GBF1, the three human large ArfGEFs, revealed that BIG1 is required to maintain the normal morphology of the Golgi complex and BIG2 is essential for endosomal compartment integrity (Boal and Stephens, 2010).

In vivo function of Garz

Homologues of Garz were identified in all eukaryotes in the course of genome projects; however, their in vivo role was analyzed only in *Arabidopsis thaliana* and in *Saccharomyces cerevisiae*. Mutations in the *Arabidopsis* paralogues GNOM and

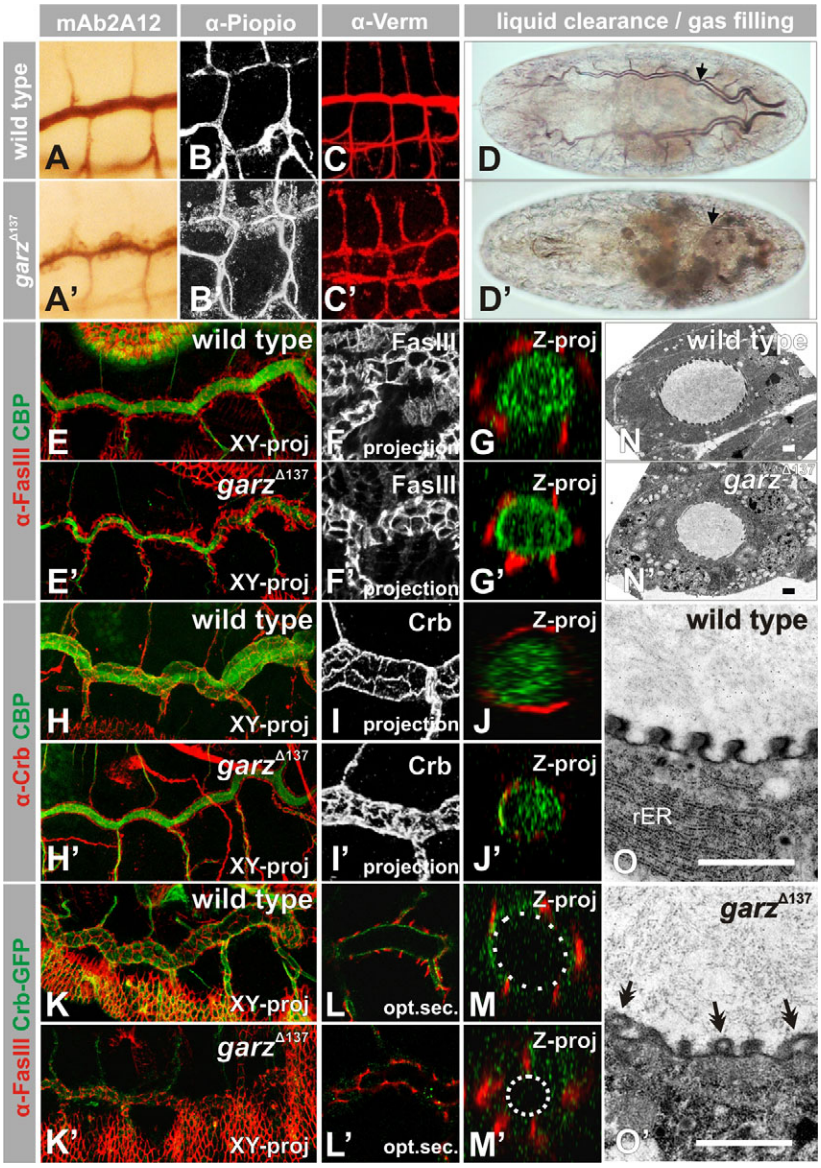

Fig. 5. Garz is required for luminal matrix deposition in tracheal cells. (**A–C**,**A′–C′**) To visualize matrix deposition in wild-type (A–C) and *garz*$^{\Delta 137}$ mutant (A–A′) embryos, we stained for 2A12 (A,A′), Piopio (B, B′), Verm (C,C′). Luminal deposition defects and protein retention in intracellular compartments, accompanied by a reduced luminal diameter are apparent in *garz* mutant embryos. (**D**,**D′**) The clearance of liquid and replacement with gas are visible in wild-type animals at late stage 16 (D) but is inhibited in *garz* mutants (D′). The dorsal trunk is indicated by an arrow. See also supplementary material Movies 1 and 2. (**E–G′**) The morphology of septate junctions marked by FasIII in *garz* embryos (E′,F′,G′) appears similar to those in wild-type embryos (E,F,G). Embryos were co-stained with CBP (chitin binding probe). (**H–J′**) Compared with wild-type cells (H,I,J) the apical membrane domains of tracheal cells in *garz* mutant embryos (H′,I′,J′; marked by Crb) are irregular and smaller. Embryos were co-stained with CBP. (**K–M′**) Co-staining for Crb–GFP (Huang et al., 2009) and FasIII revealed that endogenous Crb–GFP in *garz* mutants (K′,L′,M′) is not restricted to the apical membrane, as seen in the wild type (K,L,M). (**N–O′**) TEM micrographs of trachea from wild-type (N,O) and *garz*$^{\Delta 137}$ mutant embryos (N′ and O′) reveal severe morphological defects in cellular compartments in *garz* mutants (see O and O′ for enlargements). The numerous elliptic or round structures seen in tracheal cells of *garz* mutants are malformed ER. The tenidiae (marked by double arrows) that form the inner ridge of the dorsal trunk are deformed and hollow. Note the absence of a proper endomembrane system (especially rough ER beneath the apical membrane) in *garz* mutants (compare O and O′). Scale bars: 1 μm.

GNOM-like (GNL1) lead to impaired auxin transport, caused by the requirement of GNOM for correct polar localization of PIN1, a crucial efflux facilitator for auxin (Bonifacino and Jackson, 2003; Geldner et al., 2003; Geldner et al., 2004; Richter et al., 2007; Teh and Moore, 2007). In budding yeast, two paralogous genes for Gartenzwerg are present, namely Gea1 and Gea2. Double mutants are lethal, causing failure to bud, and the dying cells show severe defects in the organization of the actin cytoskeleton (Peyroche et al., 2001; Spang et al., 2001; Zakrzewska et al., 2003).

As reported in this study, in *Drosophila* the morphologies of both the ER and Golgi complex clearly depend on Garz. Our TEM analysis of highly active secretory cells in salivary glands revealed a considerable expansion of the ER lumen and many fewer Golgi-derived vesicles in *garz* mutant animals. Secretory vesicles that normally accumulate close to the apical membrane and subsequently release their cargo into the luminal space are virtually absent in *garz* mutants. Instead, an accumulation of electron-dense material on the basal side of salivary gland cells is visible, which is accompanied by a large number of apparently empty vesicles. Therefore, we postulate that Garz interferes with the secretory pathway of the cells. This interpretation of our results is in agreement with previous studies that have established Garz as a major component of the Arf1–COPI secretory pathway. Blocking Arf1–COPI either in budding yeast, cultured mammalian cells or in *Drosophila* mutants causes a progressive disassembly of the Golgi with its components being redistributed back to the ER. In addition, mutations in Arf1–COPI hinder the transport of secretory vesicles towards the plasma membrane. Similarly, inhibition of the Sar1–COPII machinery (Förster et al., 2010; Norum et al., 2010; Tsarouhas et al., 2007) also causes disassembly of the Golgi complex and cargo fails to reach its correct membrane destination (Ward et al., 2001). In the absence of functional Garz, the activation of Arf1, which is involved in the formation and function of COPI complexes, fails, eventually leading to the disruption of one or several trafficking routes. This idea is corroborated by our findings that several proteins known to be transported either to distinct membrane compartments or

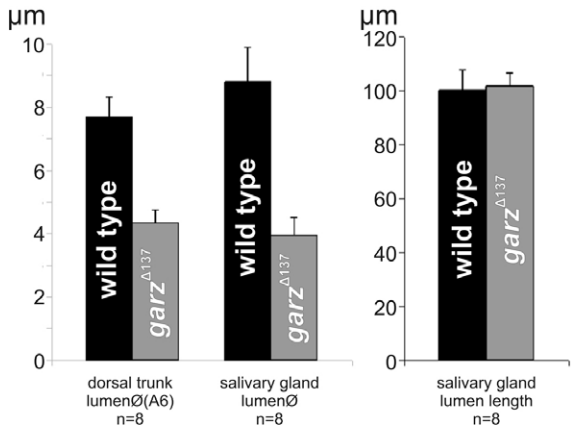

Fig. 6. Luminal diameter. The graph shows the luminal diameter and the total length of salivary glands and the luminal diameter of trachea (dorsal trunk, segment A6) of stage 16–17 wild-type and *garz* mutant embryos. Measurements were made from confocal image stacks of embryos stained for Crb, and the length measuring function provided in the Zeiss LSM software package. The luminal diameter in *garz* mutants was significantly smaller ($P<0.001$) than in wild-type embryos, but the total lengths were similar.

secreted into the lumen or to cuticle structures, are retained inside the cell and accumulate in vesicular compartments. We conclude that the phenotypes seen in *garz* mutants on the cellular and ultrastructural level are consistent with the function of the protein as a guanine nucleotide exchange factor for Arf1 in the Arf1–COPI secretory pathway machinery.

Furthermore, we found that animals lacking *garz* suffer from morphological defects in lumen formation in salivary glands and trachea. Although the formation of biological tubes is mechanistically different in these tissues (Baer et al., 2009), apical membrane and luminal matrix expansion probably play a general role in tube formation. Garz might be directly involved in these processes through its known ability to convert Arf1 from an inactive into an active state (Kawamoto et al., 2002; Szul et al., 2005; Zhao et al., 2002). On the one hand, activated Arf1 regulates COPI coat assembly and vesicle budding at the Golgi membrane. Disruption of this process impairs the proper delivery of secreted components or membrane regulators to their physiological destinations, e.g. the expanding lumen of salivary glands. On the other hand, Arf1 modulates Golgi structure by stimulating the assembly of Spectrin and Actin cytoskeletal elements at Golgi membranes (Fucini et al., 2002; Fucini et al., 2000; Godi et al., 1998). In *garz* mutants ARF1 presumably remains inactive, which ultimately leads to the disassembly of Golgi architecture. Such an idea is in agreement with studies demonstrating that mutations affecting COPI coatomers γ-COP and δ-COP (Grieder et al., 2008; Jayaram et al., 2008), COPII coatomers Sec23 and Sec24 (Förster et al., 2010; Norum et al., 2010) and Sar1 (Tsarouhas et al., 2007) compromise ER and Golgi morphology and additionally cause severe defects in tube expansion in salivary glands and trachea. Our finding that *garz* mutants affect the delivery of luminal matrix components and thereby cause luminal diameter reduction is also in agreement with previous studies that have shown that, for example, α-subunits of resident ER enzymes PH4αSG1 and PH4βSG1, which are hydroxylate proline residues in procollagen and other secreted proteins, are responsible for altered salivary gland secretion causing regional tube dilation and constriction, with intermittent tube closure (Abrams et al., 2006). Although tracheal lumen formation is mechanistically distinct from lumen formation in salivary glands, *garz* mutations lead to perturbed lumen dilation also in this tissue. As a direct consequence of loss of Garz activity, the transport vesicles carrying lipids for apical membrane growth and transient luminal proteins are not able to be targeted to the luminal side. Thus, protein secretion into the lumen and incorporation into the apical membrane is severely disturbed.

Recently it was shown that Garz has a function in the endosomal system (Gupta et al., 2009). The authors provided evidence, that Garz is required for the Arf1-dependent fluid uptake mediated by the clathrin- and dynamin-independent GEEC pathway. After internalization, GEEC endosomes fuse with Rab5-containing endosomes. Initially, GEEC endosomes are mainly devoid of early endosomal markers such as Rab5 and EEA1 (Kalia et al., 2006). This is in accordance with our observation that Garz and Rab5 cofractionate only to a very limited amount (Fig. 2C), indicating, that Garz might play a role in early steps of the GEEC pathway rather than being associated with other endosomal pathways. Although speculative, it might be that Garz and the GEEC pathway are required for fluid uptake upon tracheal liquid clearance.

Our analysis of *garz* loss-of-function mutants led us to conclude that Garz is essential to initiate assembly of the Arf1–COPI machinery and to maintain the integrity of the Golgi complex. In the secretory pathway, lack of intact Golgi and COPI-vesicle formation leads to failure in directed cargo export and accumulation of cargo within and at the ER, which is in agreement with the previously proposed models (Ward et al., 2001). During organogenesis, lack of Garz becomes manifested primarily in tubular organs and epithelial structures, which are strongly impaired.

Materials and Methods

Fly stocks and genetics

The wild-type strain used was *white*^{1118}. The EMS allele S4-50 was generated in the lab of C. Klämbt (Hummel et al., 1999) and identified by us in a genetic screen for heart mutants (Albrecht et al., 2006). The EMS-induced mutant *garz*^{EMS667} was generated in the laboratory of G. Technau and identified in a screen for nervous system mutants and verified as a *garz* allele in this study and by O. Vef and B. Altenhein (Vef et al., 2006). The *garz*$^{EP(2)2028}$ allele was generated in P. Rørth's lab and obtained from the Szeged Stock Center (Rørth, 1996). The EPgy2^{EY07592} P-element line was generated by the *Drosophila* genome project (Bellen et al., 2004) and provided by the Bloomington Stock Center. All other lines were obtained from the Bloomington Stock Center. We used the Bloomington deficiency kit (released March 2005) and the DrosDel isogenic core deletion kit (Ryder et al., 2004) for mapping of the EMS-induced alleles.

The homozygous viable P-element insertion line EPgy2^{EY07592} was used to generate *garz* mutations by imprecise excision. EPgy2^{EY07592} (w^+ mc, light orange eyes) was mobilized as follows: 100 *y w*^{1118}; EPgy2^{EY07592} virgin females were crossed to jump starter males *y w*^{1118}; PBac$^{\Delta 2-3}$ (w^+ red eyes). Resulting *y w*^{1118}; EPgy2^{EY07592}/PBac$^{\Delta 2-3}$ males (100) were individually crossed to *y w*^{1118}; If/CyO, kr–GFP virgin females. Individual white eyed males from the F2 generation (100) were selected and crossed back to *y w*^{1118}; If/CyO, kr–GFP females to establish stocks. We tested ~800 lethal jump out lines for complementation with Df(2R)Exel6061 in which *garz* is absent. Lines that failed to complement Df(2R)Exel6061 were kept for further analysis. The newly induced stocks fall into two complementation groups. One group turned out to be allelic to the EMS-induced mutant alleles S4-50 and EMS667, and to the EP(2)2028. We sequenced genomic DNA isolated from theses alleles to determine the deletion breakpoint (see Result section). The second complementation group is allelic to the larger deficiency Df(2R)Exel6061 but not to *garz* alleles. Sequencing of genomic DNA isolated from alleles belonging to this second complementation group revealed that they carry deletions with breakpoints mapping to the original EP-element insertion site and within the gene CG8841. These alleles were not further characterized. For lethal phase determination we balanced *garz* alleles over CyO, *kr*–GFP.

Homozygous mutant individuals were identified by the absence of GFP expression. A knock-in line carrying a Crumbs-GFP fusion protein was obtained from Y. Hong (University of Pittsburgh) (Huang et al., 2009).

Molecular biology

A cDNA containing the whole open reading frame of *garz* was amplified from isolated total RNA from Oregon-R flies using the SuperScript One-Step RT-PCR system and subsequently cloned into pCR2.1-TOPO vector (Invitrogen, Carlsbad, CA). Primers used were: forward: 5′-ATGGCGCTTCCAGGCAACG-3′ and reverse: 5′-TCACTGCTGGCCGTAGAGCA-3′. To determine the EMS-induced point mutations in $garz^{S4\text{-}50}$ and $garz^{EMS667}$, we isolated genomic DNA from heterozygous adult flies or selected homozygous mutant embryos. PCR amplicons were cloned and sequenced twice in both directions. To distinguish between polymorphisms and EMS-induced point mutations, we amplified and sequenced corresponding gene regions from EMS alleles from the same mutant collection with isogenic background in parallel ($kuz^{J2\text{-}11}$, $mam^{S2\text{-}29}$) (Albrecht et al. 2006).

In situ hybridization for *garz* mRNA

For probe synthesis we cloned a 1937 bp fragment (nucleotides 302–2268) of the full-length *garz* cDNA into the pGEM-T easy cloning vector (Promega, Madison, WI) using the following primers: forward 5′-ATCCCACGTCTCCAAATCTGG-3′, and reverse 5′-ATGCCAATGATCAGAAAAGTG-3′. Sense and anti-sense RNA probes were synthesized using the DIG RNA Labelling Kit (Roche, Basel, Switzerland). In situ hybridization and double labelling with antibodies were performed as described previously (Duan et al., 2001).

Antibody production

A 939 bp cDNA fragment encoding amino acids 1368–1680 of the predicted isoform A was cloned into the pET16b vector and transformed into *Escherichia coli* Rosetta (DE3) cells (Novagen, EMD Biosciences, Madison, WI). The sequences of the respective primers were: forward 5′-TACTCACATAT-GCGCTGCATCCGCATCTTT-3′ GTG, and reverse 5′-TACTCGGGATCC-TCTAATTTGCGTATAGTCAAG-3′. Expression was done essentially as previously described (Meyer et al., 2009) and the refolded protein (fused to a N-terminal 10xHis tag) was purified using Ni-NTA Agarose (Qiagen, Hilden, Germany) according to the manufacturer's instructions. Finally the antigen was used for immunization of two rabbits (Pineda Antibody Service, Berlin, Germany). To improve specificity, the resulting sera were purified by antigen affinity, and the monospecificity was confirmed by western blotting.

S2 cell culture and subcellular fractionation

S2 cells were grown in Schneider's *Drosophila* medium supplemented with L-glutamine (Invitrogen) in 175 cm^2 flasks to 95% confluency and harvested by centrifugation (100 ***g***, 10 minutes). Cell were disrupted in PBS supplemented with Protease-Inhibitor Mix M (Serva, Heidelberg, Germany), by the freeze–thaw method and the coarse protein extract was centrifuged at 2000 ***g*** for 10 minutes to remove cell debris and nuclei. The resulting postnuclear supernatant was then layered onto a 0.3–2.0 M linear sucrose gradient and centrifuged at 36,000 r.p.m. (160,000 ***g***) for 18 hours using a SW 41 Ti rotor (Beckman Coulter, Brea, CA). A total of 12 fractions of 1 ml each were collected from the bottom of the tube and analyzed by SDS-polyacrylamide gel electrophoresis and western blot analysis using anti-Garz antibody and the following antibodies for the indicated membrane compartments: anti-GM130 (*cis*-Golgi) and anti-Rab5 (early endosomes).

Yeast

Garz-RB and Gea1 cDNAs were tagged with a yeast EGFP (Sheff and Thorn, 2004) at the C-terminus using PCR-based homologous recombination, and stably integrated at the *gea1* locus by homologous recombination using standard techniques (cloning details available upon request). For colocalization studies we used a strain that carries the *cis*-Golgi protein Mnn9 (Jungmann and Munro, 1998) fused to the td-Tomato cassette (Meiringer et al., 2008). Tetrad analyses of the diploid strains were followed by succeeding selections on appropriate media for haploid segregants producing either Gea1–EGFP or Garz–EGFP together with Mnn9–td-Tomato.

Immunohistochemistry and transmission electron microscopy

Whole-mount immunostainings were carried out as described previously (Albrecht et al., 2011). Embryos were collected from grape juice agar plates and dechorionated in 50% DanKlorix (Colgate Palmolive), then fixed in a 1:1 (v/v) mixture of PBS, containing 50 mM EGTA and freshly prepared methanol-free 9% formaldehyde (Polysciences Inc., Eppelheim, Germany) and *n*-heptane for 30 minutes at room temperature. Devitellinisation was performed by shaking for 60 seconds in 1:1 (v/v) mixture of methanol and *n*-heptane. Confocal images were captured either with a Zeiss LSM 5 Pascal confocal microscope or a Leica SP1 confocal microscope. Z-stacks are depicted as maximum projections if not denoted otherwise. Whole-mount in situ hybridizations were documented with a Zeiss AxioCam MRc5 camera mounted on a Zeiss Axioskop 2, whereas immunofluorescence and live cell imaging of yeast and S2 cells were undertaken with a cooled CCD CoolSNAP HQ camera on a Zeiss Axioplan 2 then processed with MetaMorph v.6.2 software. For TEM analysis, embryos were prepared as described previously (Lehmacher et al., 2009; Tepass and Hartenstein, 1994). After fixation, the specimens were embedded in Epon 812, and ultra-thin sections (70 nm) were cut for TEM with a diamond knife on a Leica Ultracut UCT ultramicrotome. Sections were mounted on single slot grids, contrasted with uranyl acetate (40 minutes; 20℃) and lead citrate (6 minutes; 20℃) using a Leica EMstain. Specimens were examined with a Zeiss 902 transmission electron microscope (60 kV).

Antibodies and reagents

Monoclonal antibodies for Crumbs (mAbCq4, 1:100); Dlg (4F3, supernatant 1:10); FasIII (7G10; supernatant 1:10) and Pericardin (EC11, 1:100) were obtained from the Hybridoma Bank, University of Iowa. Monoclonal mouse anti-galactosidase (Z378B; 1:5000) was from Promega; monoclonal mouse anti-GFP (3E6; 1:1000) was from Invitrogen (A11120); polyclonal antibodies for GM130 and Rab5 were from Abcam (ab30637, ab31261; 1:100). The polyclonal rabbit anti-Pio antibody (Jazwinska et al., 2003) was used at a dilution of 1:200, the polyclonal rabbit anti-Verm (Luschnig et al., 2006) at 1:100, polyclonal rabbit anti-Bazooka at 1:1000 (Wodarz et al., 1999). The polyclonal mouse anti-AP1 (Benhra et al., 2011) was used at a dilution of 1:300, the polyclonal rat anti-GCC185 (Sinka et al., 2008) at a dilution of 1:100 and the polyclonal mouse anti-MHC at a dilution of 1:500 (Kiehart, 1990). Monoclonal mouse IgM 2A12 was kindly provided by Nipam Patel (University of California at Berkeley) and used at 1:10 with the Vectastain Kit from Vector Laboratories. The anti-Garz, described in this study, was used at a dilution of 1:100. Secondary antibodies coupled with Cy2 or Cy3 were obtained from Dianova (Pinole, CA). Fluorescein-conjugated chitin-binding probe (CBP) from New England Biolabs (P5211S; Ipswich, MA) was kindly provided by R. Schuh (Max Planck Institute for Biophysical Chemistry, Göttingen) and used at a dilution of 1:500.

Cuticle preparation

Cuticles were prepared as described previously (Alexandre, 2008), with minor modifications. Briefly, embryos between 0 and 6 hours AED (after egg deposition) were collected and aged for an additional 24–36 hours at 25℃. Then, mobile larvae were removed from the agar plate. the remaining specimens were fixed in 4% formaldehyde. For cuticle preparation, a mixture consisting of 50% Hoyer's mountant and 50% lactic acid was used. The specimens were incubated at 60℃ for 72 hours before mounting on a microscope slide for examination using dark-field microscopy.

Acknowledgements

We thank C. Klämbt, R. Le Borgne, S. Goto, Y. Hong, S. Luschnig, S. Munro, N. Patel, R. Schuh, G. Technau, C. Ungermann and A. Wodarz for sharing fly stocks or reagents, O. Vef for initial mapping of the $garz^{EMS667}$ allele, S. Tejedor Vaquero for assisting DNA sequence analysis, and S. Vos for generating the time-lapse movie. We also thank K. Etzold for her assistance with TEM analysis, and E. Haß-Cordes, M. Krabusch and M. Biedermann for excellent technical support.

Funding

This work was supported by the Deutsche Forschungsgemeinschaft within the framework of the SFB 431 and SFB 944 to A.P. and to J.J.H. A.O. and M.A. were supported by SystemsX.ch within the framework of the WingX RTD, the Swiss National Science Foundation and the Kantons of Basel-Stadt and Basel-Land.

Supplementary material available online at
http://jcs.biologists.org/lookup/suppl/doi:10.1242/jcs.092551/-/DC1

References

Abrams, E. W., Mihoulides, W. K. and Andrew, D. J. (2006). Fork head and Sage maintain a uniform and patent salivary gland lumen through regulation of two downstream target genes, PH4alphaSG1 and PH4alphaSG2. *Development* **133**, 3517-3527.

Affolter, M. and Caussinus, E. (2008). Tracheal branching morphogenesis in *Drosophila:* new insights into cell behaviour and organ architecture. *Development* **135**, 2055-2064.

Albrecht, S., Wang, S., Holz, A., Bergter, A. and Paululat, A. (2006). The ADAM metalloprotease Kuzbanian is crucial for proper heart formation in *Drosophila melanogaster*. *Mech. Dev.* **123**, 372-387.

Albrecht, S., Altenhein, B. and Paululat, A. (2011). The transmembrane receptor Uncoordinated5 (Unc5) is essential for heart lumen formation in *Drosophila melanogaster*. *Dev. Biol.* **350**, 89-100.

Alexandre, C. (2008). Cuticle preparation of *Drosophila* embryos and larvae. In *Drosophila: Methods and Protocols*, Vol. 420 (ed. C. Dahmann), pp. 97-205. Totowa: Humana Press.

Andrew, D. J. and Ewald, A. J. (2010). Morphogenesis of epithelial tubes: Insights into tube formation, elongation, and elaboration. *Dev. Biol.* **341**, 34-55.

Arquier, N., Geminard, C., Bourouis, M., Jarretou, G., Honegger, B., Paix, A. and Leopold, P. (2008). *Drosophila* ALS regulates growth and metabolism through functional interaction with insulin-like peptides. *Cell Metab.* **7**, 333-338.

Baer, M. M., Chanut-Delalande, H. and Affolter, M. (2009). Cellular and molecular mechanisms underlying the formation of biological tubes. *Curr. Top. Dev. Biol.* **89**, 137-162.

Bard, F., Casano, L., Mallabiabarrena, A., Wallace, E., Saito, K., Kitayama, H., Guizzunti, G., Hu, Y., Wendler, F., Dasgupta, R. et al. (2006). Functional genomics reveals genes involved in protein secretion and Golgi organization. *Nature* **439**, 604-607.

Behr, M., Wingen, C., Wolf, C., Schuh, R. and Hoch, M. (2007). Wurst is essential for airway clearance and respiratory-tube size control. *Nat. Cell Biol.* **9**, 847-853.

Bellen, H. J., Levis, R. W., Liao, G., He, Y., Carlson, J. W., Tsang, G., Evans-Holm, M., Hiesinger, P. R., Schulze, K. L., Rubin, G. M. et al. (2004). The BDGP gene disruption project: single transposon insertions associated with 40% of *Drosophila* genes. *Genetics* **167**, 761-781.

Beller, M., Sztalryd, C., Southall, N., Bell, M., Jäckle, H., Auld, D. S. and Oliver, B. (2008). COPI complex is a regulator of lipid homeostasis. *PLoS Biol.* **6**, e292.

Benhra, N., Lallet, S., Cotton, M., Le Bras, S., Dussert, A. and Le Borgne, R. (2011). AP-1 controls the trafficking of Notch and Sanpodo toward E-cadherin junctions in sensory organ precursors. *Curr. Biol.* **21**, 87-95.

Boal, F. and Stephens, D. J. (2010). Specific functions of BIG1 and BIG2 in endomembrane organization. *PLoS ONE* **5**, e9898.

Bökel, C., Prokop, A. and Brown, N. H. (2005). Papillote and Piopio: *Drosophila* ZP-domain proteins required for cell adhesion to the apical extracellular matrix and microtubule organization. *J. Cell Sci.* **118**, 633-642.

Bonifacino, J. S. and Jackson, C. L. (2003). Endosome-specific localization and function of the ARF activator GNOM. *Cell* **112**, 141-142.

Bryant, D. M. and Mostov, K. E. (2008). From cells to organs: building polarized tissue. *Nat. Rev. Mol. Cell Biol.* **9**, 887-901.

Chantalat, S., Courbeyrette, R., Senic-Matuglia, F., Jackson, C. L., Goud, B. and Peyroche, A. (2003). A novel Golgi membrane protein is a partner of the ARF exchange factors Gea1p and Gea2p. *Mol. Biol. Cell* **14**, 2357-2371.

Chung, S. and Andrew, D. J. (2008). The formation of epithelial tubes. *J. Cell Sci.* **121**, 3501-3504.

Claude, A., Zhao, B. P., Kuziemsky, C. E., Dahan, S., Berger, S. J., Yan, J. P., Armold, A. D., Sullivan, E. M. and Melancon, P. (1999). GBF1: A novel Golgi-associated BFA-resistant guanine nucleotide exchange factor that displays specificity for ADP-ribosylation factor 5. *J. Cell Biol.* **146**, 71-84.

de Wit, M. C., de Coo, I. F., Halley, D. J., Lequin, M. H. and Mancini, G. M. (2009). Movement disorder and neuronal migration disorder due to ARFGEF2 mutation. *Neurogenetics* **10**, 333-336.

Duan, H., Skeath, J. B. and Nguyen, H. T. (2001). *Drosophila* Lame duck, a novel member of the Gli superfamily, acts as a key regulator of myogenesis by controlling fusion-competent myoblast development. *Development* **128**, 4489-4500.

Förster, D., Armbruster, K. and Luschnig, S. (2010). Sec24-dependent secretion drives cell-autonomous expansion of tracheal tubes in *Drosophila*. *Curr. Biol.* **20**, 62-68.

Fucini, R. V., Navarrete, A., Vadakkan, C., Lacomis, L., Erdjument-Bromage, H., Tempst, P. and Stamnes, M. (2000). Activated ADP-ribosylation factor assembles distinct pools of actin on golgi membranes. *J. Biol. Chem.* **275**, 18824-18829.

Fucini, R. V., Chen, J. L., Sharma, C., Kessels, M. M. and Stamnes, M. (2002). Golgi vesicle proteins are linked to the assembly of an actin complex defined by mAbp1. *Mol. Biol. Cell* **13**, 621-631.

Geldner, N., Anders, N., Wolters, H., Keicher, J., Kornberger, W., Muller, P., Delbarre, A., Ueda, T., Nakano, A. and Jürgens, G. (2003). The *Arabidopsis* GNOM ARF-GEF mediates endosomal recycling, auxin transport, and auxin-dependent plant growth. *Cell* **112**, 219-230.

Geldner, N., Richter, S., Vieten, A., Marquardt, S., Torres-Ruiz, R. A., Mayer, U. and Jürgens, G. (2004). Partial loss-of-function alleles reveal a role for GNOM in auxin transport-related, post-embryonic development of *Arabidopsis*. *Development* **131**, 389-400.

Gillingham, A. K. and Munro, S. (2007). The small G proteins of the Arf family and their regulators. *Annu. Rev. Cell Dev. Biol.* **23**, 579-611.

Godi, A., Santone, I., Pertile, P., Devarajan, P., Stabach, P. R., Morrow, J. S., Di Tullio, G., Polishchuk, R., Petrucci, T. C., Luini, A. et al. (1998). ADP ribosylation factor regulates spectrin binding to the Golgi complex. *Proc. Natl. Acad. Sci. USA* **95**, 8607-8612.

Grieder, N. C., Caussinus, E., Parker, D. S., Cadigan, K., Affolter, M. and Luschnig, S. (2008). gammaCOP is required for apical protein secretion and epithelial morphogenesis in *Drosophila melanogaster*. *PLoS ONE* **3**, e3241.

Guo, Y., Walther, T. C., Rao, M., Stuurman, N., Goshima, G., Terayama, K., Wong, J. S., Vale, R. D., Walter, P. and Farese, R. V. (2008). Functional genomic screen reveals genes involved in lipid-droplet formation and utilization. *Nature* **453**, 657-661.

Gupta, G. D., Swetha, M. G., Kumari, S., Lakshminarayan, R., Dey, G. and Mayor, S. (2009). Analysis of endocytic pathways in *Drosophila* cells reveals a conserved role for GBF1 in internalization via GEECs. *PLoS ONE* **4**, e6768.

Huang, J., Zhou, W., Dong, W., Watson, A. M. and Hong, Y. (2009). Directed, efficient, and versatile modifications of the *Drosophila* genome by genomic engineering. *Proc. Natl. Acad. Sci. USA* **106**, 8284-8289.

Hummel, T., Schimmelpfeng, K. and Klämbt, C. (1999). Commissure formation in the embryonic CNS of *Drosophila*. *Dev. Biol.* **209**, 381-398.

Jayaram, S. A., Senti, K. A., Tiklova, K., Tsarouhas, V., Hemphala, J. and Samakovlis, C. (2008). COPI vesicle transport is a common requirement for tube expansion in *Drosophila*. *PLoS ONE* **3**, e1964.

Jazwinska, A., Ribeiro, C. and Affolter, M. (2003). Epithelial tube morphogenesis during *Drosophila* tracheal development requires Piopio, a luminal ZP protein. *Nat. Cell Biol.* **5**, 895-901.

Jungmann, J. and Munro, S. (1998). Multi-protein complexes in the cis Golgi of *Saccharomyces cerevisiae* with alpha-1,6-mannosyltransferase activity. *EMBO J.* **17**, 423-434.

Kahn, R. A. and Gilman, A. G. (1986). The protein cofactor necessary for ADP-ribosylation of Gs by cholera toxin is itself a GTP binding protein. *J. Biol. Chem.* **261**, 7906-7911.

Kalia, M., Kumari, S., Chadda, R., Hill, M. M., Parton, R. G. and Mayor, S. (2006). Arf6-independent GPI-anchored protein-enriched early endosomal compartments fuse with sorting endosomes via a Rab5/phosphatidylinositol-3′-kinase-dependent machinery. *Mol. Biol. Cell* **17**, 3689-3704.

Kawamoto, K., Yoshida, Y., Tamaki, H., Torii, S., Shinotsuka, C., Yamashina, S. and Nakayama, K. (2002). GBF1, a guanine nucleotide exchange factor for ADP-ribosylation factors, is localized to the cis-Golgi and involved in membrane association of the COPI coat. *Traffic* **3**, 483-495.

Kiehart, D. P. (1990). Molecular genetic dissection of myosin heavy chain function. *Cell* **60**, 347-350.

Kraut, R., Menon, K. and Zinn, K. (2001). A gain-of-function screen for genes controlling motor axon guidance and synaptogenesis in *Drosophila*. *Curr. Biol.* **11**, 417-430.

LaJeunesse, D. R., Buckner, S. M., Lake, J., Na, C., Pirt, A. and Fromson, K. (2004). Three new *Drosophila* markers of intracellular membranes. *Biotechniques* **36**, 784-788, 790.

Lee, M. C., Miller, E. A., Goldberg, J., Orci, L. and Schekman, R. (2004). Bi-directional protein transport between the ER and Golgi. *Annu. Rev. Cell Dev. Biol.* **20**, 87-123.

Lehmacher, C., Tögel, M., Pass, G. and Paululat, A. (2009). The *Drosophila* wing hearts consist of syncytial muscle cells that resemble adult somatic muscles. *Arthropod Struct. Dev.* **38**, 111-123.

Luschnig, S., Batz, T., Armbruster, K. and Krasnow, M. A. (2006). *serpentine* and *vermiform* encode matrix proteins with chitin binding and deacetylation domains that limit tracheal tube length in *Drosophila*. *Curr. Biol.* **16**, 186-194.

Maybeck, V. and Röper, K. (2009). A targeted gain-of-function screen identifies genes affecting salivary gland morphogenesis/tubulogenesis in *Drosophila*. *Genetics* **181**, 543-565.

Meiringer, C. T., Auffarth, K., Hou, H. and Ungermann, C. (2008). Depalmitoylation of Ykt6 prevents its entry into the multivesicular body pathway. *Traffic* **9**, 1510-1521.

Meyer, H., Panz, M., Zmojdzian, M., Jagla, K. and Paululat, A. (2009). Neprilysin 4, a novel endopeptidase from *Drosophila melanogaster*, displays distinct substrate specificities and exceptional solubility states. *J. Exp. Biol.* **212**, 3673-3683.

Mouratou, B., Biou, V., Joubert, A., Cohen, J., Shields, D. J., Geldner, N., Jürgens, G., Melancon, P. and Cherfils, J. (2005). The domain architecture of large guanine nucleotide exchange factors for the small GTP-binding protein Arf. *BMC Genomics* **6**, 20.

Nakamura, N., Rabouille, C., Watson, R., Nilsson, T., Hui, N., Slusarewicz, P., Kreis, T. E. and Warren, G. (1995). Characterization of a cis-Golgi matrix protein, GM130. *J. Cell Biol.* **131**, 1715-1726.

Niu, T. K., Pfeifer, A. C., Lippincott-Schwartz, J. and Jackson, C. L. (2005). Dynamics of GBF1, a Brefeldin A-sensitive Arf1 exchange factor at the Golgi. *Mol. Biol. Cell* **16**, 1213-1222.

Norum, M., Tang, E., Chavoshi, T., Schwarz, H., Linke, D., Uv, A. and Moussian, B. (2010). Trafficking through COPII stabilises cell polarity and drives secretion during *Drosophila* epidermal differentiation. *PLoS ONE* **5**, e10802.

Peyroche, A. and Jackson, C. L. (2001). Functional analysis of ADP-ribosylation factor (ARF) guanine nucleotide exchange factors Gea1p and Gea2p in yeast. *Methods Enzymol.* **329**, 290-300.

Peyroche, A., Courbeyrette, R., Rambourg, A. and Jackson, C. L. (2001). The ARF exchange factors Gea1p and Gea2p regulate Golgi structure and function in yeast. *J. Cell Sci.* **114**, 2241-2253.

Ramaen, O., Joubert, A., Simister, P., Belgareh-Touze, N., Olivares-Sanchez, M. C., Zeeh, J. C., Chantalat, S., Golinelli-Cohen, M. P., Jackson, C. L., Biou, V. et al. (2007). Interactions between conserved domains within homodimers in the big1, big2 and GBF1 ARF guanine nucleotide exchange factors. *J. Biol. Chem.* **282**, 28834-28842.

Richter, S., Geldner, N., Schrader, J., Wolters, H., Stierhof, Y. D., Rios, G., Koncz, C., Robinson, D. G. and Jürgens, G. (2007). Functional diversification of closely related ARF-GEFs in protein secretion and recycling. *Nature* **448**, 488-492.

Rørth, P. (1996). A modular misexpression screen in *Drosophila* detecting tissue-specific phentoypes. *Proc. Natl. Acad. Sci. USA* **93**, 12418-12422.

Ryder, E., Blows, F., Ashburner, M., Bautista-Llacer, R., Coulson, D., Drummond, J., Webster, J., Gubb, D., Gunton, N., Johnson, G. et al. (2004). The DrosDel collection: a set of P-element insertions for generating custom chromosomal aberrations in *Drosophila melanogaster*. *Genetics* **167**, 797-813.

Sáenz, J. B., Sun, W. J., Chang, J. W., Li, J., Bursulaya, B., Gray, N. S. and Haslam, D. B. (2009). Golgicide A reveals essential roles for GBF1 in Golgi assembly and function. *Nat. Chem. Biol.* **5**, 157-165.

Schottenfeld, J., Song, Y. and Ghabrial, A. S. (2010). Tube continued: morphogenesis of the *Drosophila* tracheal system. *Curr. Opin. Cell Biol.* **22**, 633-639.

Sheen, V. L., Ganesh, V. S., Topcu, M., Sebire, G., Bodell, A., Hill, R. S., Grant, P. E., Shugart, Y. Y., Imitola, J., Khoury, S. J. et al. (2004). Mutations in ARFGEF2 implicate vesicle trafficking in neural progenitor proliferation and migration in the human cerebral cortex. *Nat. Genet.* **36**, 69-76.

Sheff, M. A. and Thorn, K. S. (2004). Optimized cassettes for fluorescent protein tagging in *Saccharomyces cerevisiae*. *Yeast* **21**, 661-670.

Sinka, R., Gillingham, A. K., Kondylis, V. and Munro, S. (2008). Golgi coiled-coil proteins contain multiple binding sites for Rab family G proteins. *J. Cell Biol.* **183**, 607-615.

Spang, A. (2009). On vesicle formation and tethering in the ER-Golgi shuttle. *Curr. Opin. Cell Biol.* **21**, 531-536.

Spang, A., Herrmann, J. M., Hamamoto, S. and Schekman, R. (2001). The ADP ribosylation factor-nucleotide exchange factors Gea1p and Gea2p have overlapping, but not redundant functions in retrograde transport from the Golgi to the endoplasmic reticulum. *Mol. Biol. Cell* **12**, 1035-1045.

Strilic, B., Kucera, T. and Lammert, E. (2010). Formation of cardiovascular tubes in invertebrates and vertebrates. *Cell. Mol. Life Sci.* **67**, 3209-3218.

Swanson, L. E., Yu, M., Nelson, K. S., Laprise, P., Tepass, U. and Beitel, G. J. (2009). *Drosophila convoluted/dALS* is an essential gene required for tracheal tube morphogenesis and apical matrix organization. *Genetics* **181**, 1281-1290.

Szul, T., Garcia-Mata, R., Brandon, E., Shestopal, S., Alvarez, C. and Sztul, E. (2005). Dissection of membrane dynamics of the ARF-guanine nucleotide exchange factor GBF1. *Traffic* **6**, 374-385.

Szul, T., Grabski, R., Lyons, S., Morohashi, Y., Shestopal, S., Lowe, M. and Sztul, E. (2007). Dissecting the role of the ARF guanine nucleotide exchange factor GBF1 in Golgi biogenesis and protein trafficking. *J. Cell Sci.* **120**, 3929-3940.

Szul, T., Burgess, J., Jeon, M., Zinn, K., Marques, G., Brill, J. A. and Sztul, E. (2011). The Garz Sec7 domain guanine nucleotide exchange factor for Arf regulates salivary gland development in *Drosophila*. *Cell. Logist.* **1**, 69-76.

Teh, O. K. and Moore, I. (2007). An ARF-GEF acting at the Golgi and in selective endocytosis in polarized plant cells. *Nature* **448**, 493-496.

Tepass, U. and Hartenstein, V. (1994). Epithelium formation in the Drosophila midgut depends on the interaction of endoderm and mesoderm. *Development* **120**, 579-590.

Tepass, U., Theres, C. and Knust, E. (1990). *crumbs* encodes an EGF-like protein expressed on apical membranes of *Drosophila* epithelial cells and required for organization of epithelia. *Cell* **61**, 787-799.

Tsarouhas, V., Senti, K. A., Jayaram, S. A., Tiklova, K., Hemphala, J., Adler, J. and Samakovlis, C. (2007). Sequential pulses of apical epithelial secretion and endocytosis drive airway maturation in *Drosophila*. *Dev. Cell* **13**, 214-225.

Vef, O., Cleppien, D., Löffler, T., Altenhein, B. and Technau, G. M. (2006). A new startegy for efficient *in vivo* screening of mutagenized *Drosophila* embryos. *Dev. Genes Evol.* **216**, 105-108.

Ward, T. H., Polishchuk, R. S., Caplan, S., Hirschberg, K. and Lippincott-Schwartz, J. (2001). Maintenance of Golgi structure and function depends on the integrity of ER export. *J. Cell Biol.* **155**, 557-570.

Wodarz, A., Ramrath, A., Kuchinke, U. and Knust, E. (1999). Bazooka provides an apical cue for Inscuteable localization in Drosophila neuroblasts. *Nature* **402**, 544-547.

Zakrzewska, E., Perron, M., Laroche, A. and Pallotta, D. (2003). A role for GEA1 and GEA2 in the organization of the actin cytoskeleton in *Saccharomyces cerevisiae*. *Genetics* **165**, 985-995.

Zhao, X., Lasell, T. K. and Melancon, P. (2002). Localization of large ADP-ribosylation factor-guanine nucleotide exchange factors to different Golgi compartments: evidence for distinct functions in protein traffic. *Mol. Biol. Cell* **13**, 119-133.